

LETTERS

Low-temperature oxidation of CO catalysed by Co₃O₄ nanorods

Xiaowei Xie^{1*}, Yong Li^{1*}, Zhi-Quan Liu², Masatake Haruta^{3,4} & Wenjie Shen¹

Low-temperature oxidation of CO, perhaps the most extensively studied reaction in the history of heterogeneous catalysis, is becoming increasingly important in the context of cleaning air and lowering automotive emissions^{1,2}. Hopcalite catalysts (mixtures of manganese and copper oxides) were originally developed for purifying air in submarines, but they are not especially active at ambient temperatures and are also deactivated by the presence of moisture^{3,4}. Noble metal catalysts, on the other hand, are water tolerant but usually require temperatures above 100 °C for efficient operation^{5,6}. Gold exhibits high activity at low temperatures and superior stability under moisture, but only when deposited in nanoparticulate form on base transition-metal oxides^{7–9}. The development of active and stable catalysts without noble metals for low-temperature CO oxidation under an ambient atmosphere remains a significant challenge. Here we report that tricobalt tetraoxide nanorods not only catalyse CO oxidation at temperatures as low as –77 °C but also remain stable in a moist stream of normal feed gas. High-resolution transmission electron microscopy demonstrates that the Co₃O₄ nanorods predominantly expose their {110} planes, favouring the presence of active Co³⁺ species at the surface. Kinetic analyses reveal that the turnover frequency associated with individual Co³⁺ sites on the nanorods is similar to that of the conventional nanoparticles of this material, indicating that the significantly higher reaction rate that we have obtained with a nanorod morphology is probably due to the surface richness of active Co³⁺ sites. These results show the importance of morphology control in the preparation of base transition-metal oxides as highly efficient oxidation catalysts.

Among the metal oxides, tricobalt tetraoxide is the most active for CO oxidation^{10,11}, but is severely deactivated by trace amounts of moisture (about 3–10 parts per million, p.p.m.) that are usually present in the feed gas. In fact, under dry conditions with a moisture content below 1 p.p.m., which can be obtained by passing the reaction gas through molecular-sieve traps cooled to dry-ice temperature, Co₃O₄ is intrinsically active for CO oxidation^{12,13} even below a temperature of –54 °C. However, in normal feed gas, most of the active sites of Co₃O₄ are covered by H₂O so the adsorption of CO and oxygen is appreciably hindered. Alumina-supported Co₃O₄ was reported to give 50% CO conversion at –63 °C for a normal feed gas, but the CO conversion was obtained with a transient method¹⁴ not at steady state. Here we show that Co₃O₄ nanorods can be steadily active for CO oxidation at a temperature as low as –77 °C, giving 100% CO conversion, and are quite stable even under a stream of normal feed gas containing moisture.

Nanorod-shaped Co₃O₄ was prepared by the calcination of a cobalt hydroxide carbonate precursor obtained by the precipitation of cobalt acetate with sodium carbonate in ethylene glycol. When cobalt acetate was mixed with ethylene glycol at 160 °C, the –OCH₂–CH₂O– chain

was tightly bound with the cobalt cations. The addition of aqueous sodium carbonate solution resulted in the formation of a solid cobalt hydroxide carbonate incorporating ethylene glycol, having a nanorod-shaped structure with a diameter of 10–20 nm and a length of 200–300 nm (Supplementary Fig. S1). Subsequent calcination of this precursor at 450 °C in air caused a spontaneous transformation of the morphology, forming Co₃O₄ nanorods with diameters of 5–15 nm and lengths of 200–300 nm.

Figure 1a shows a typical low-magnification transmission electron microscopy (TEM) image of the synthesized Co₃O₄, in which a batch of nanorods is developed from a cluster core, forming a coral-like morphology. Most of the nanorods have straight sides and regular ends, as shown in Fig. 1b, an enlarged TEM image. We examined the crystallographic nature of the individual Co₃O₄ nanorod using high-resolution TEM (HRTEM) observations. Figure 1c is a section of a Co₃O₄ nanorod in the [1–10] orientation, showing the growth direction as [110] and the flat side parallel to (001). These (001) side planes were also observed in the [100] orientation (Fig. 1d), which was constructed from {022} planes with a spacing of 0.286 nm. When the nanorod was tilted to the [001] zone axis (Fig. 1e), we clearly observed the two orthogonal sets of the {220} lattice. The flat top is the (110) atomic plane and the side plane is (1–10). Figure 1f shows the cross-section viewed near the [110] orientation, exhibiting a rectangular shape with the long edges parallel to (001) and the short edges parallel to (1–10). Taking all these TEM images into account, the real shape of the nanorod can be approximately reconstructed, as shown in Fig. 1g, in which the axial direction is [110]. The Co₃O₄ nanorod has two {001} flat planes, two {1–10} side planes and two {110} end planes. In other words, the Co₃O₄ nanorod mainly grows along the [110] direction and preferentially exposes the {110} plane, the surface area of which is estimated to be 41% of the total surface area.

The Co₃O₄ nanorods were tested for CO oxidation at –77 °C under a reaction stream with a gas composition of 1.0 vol.% CO/2.5 vol.% O₂/He. They showed 100% CO conversion to CO₂ during the initial 6 h; the CO conversion then tended to decrease, but only down to 80% after 12 h (Fig. 2). This catalytic performance is quite promising in terms of activity and stability when compared with the metal oxides reported thus far^{12–17}, and is even superior to supported gold nanoparticles⁷. Because Co₃O₄ is very sensitive to the presence of moisture in normal feed gas^{12,13}, we then measured the catalytic activity of the nanorods under dry conditions. Surprisingly, the CO conversion was almost the same (100%) as in the normal feed gas during the initial 6 h and there was only a slight improvement in stability during the subsequent operation (Fig. 2), suggesting that the Co₃O₄ nanorods are not very sensitive to the presence of moisture. The measured reaction rates of CO oxidation at –77 °C were $3.91 \times 10^{-6} \text{ mol g}^{-1} \text{ s}^{-1}$ for normal feed gas and $5.88 \times 10^{-6} \text{ mol g}^{-1} \text{ s}^{-1}$ under dry conditions. This indicates

¹State Key Laboratory of Catalysis, Dalian Institute of Chemical Physics, Chinese Academy of Sciences, Dalian 116023, China. ²Shenyang National Laboratory for Materials Science, Institute of Metal Research, Chinese Academy of Sciences, Shenyang 110016, China. ³Department of Applied Chemistry, Graduate School of Urban Environmental Sciences, Tokyo Metropolitan University, 1-1 Minami-osawa, Hachioji 192-0397, Tokyo, Japan. ⁴Japan Science and Technology Agency, CREST, 4-1-8 Hon-Cho, Kawaguchi 332-0012, Saitama, Japan. *These authors contributed equally to this work.

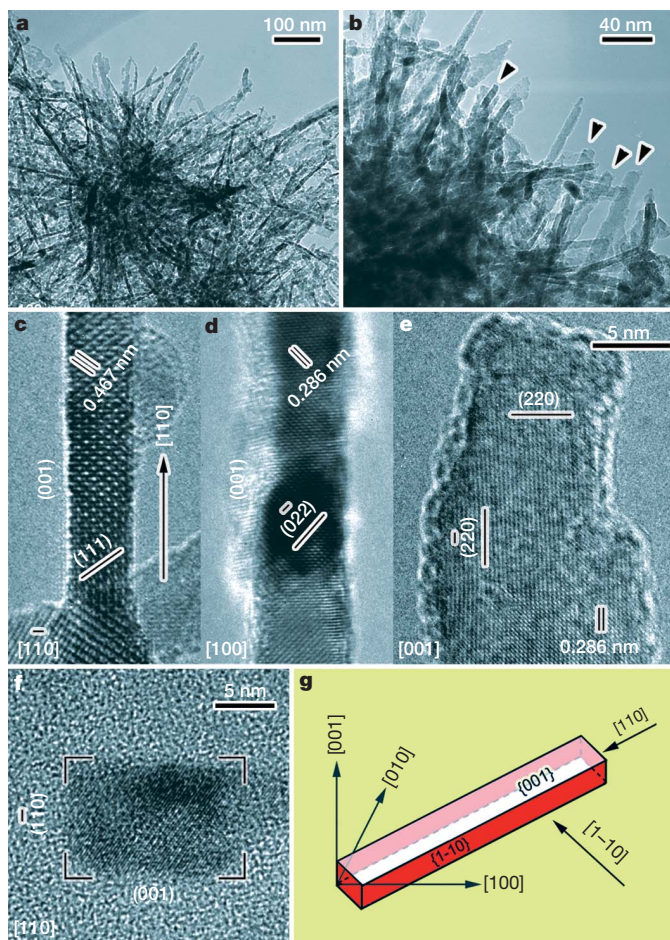


Figure 1 | TEM images of Co_3O_4 nanorods. **a, b**, Low and high magnifications, where the arrowheads indicate the straight sides and regular ends of the nanorods. **c–f**, HRTEM images viewed along the $[1-10]$ (**c**), $[100]$ (**d**), $[001]$ (**e**) and near $[110]$ (**f**) orientations. **g**, Shape of the nanorod, where red represents the catalytically active planes. Note, $[uvw]$ is an index of a specified crystal axis and (hkl) is an index of a specified crystal plane, while $\{hkl\}$ indicates a set of group crystal planes with the same atomic configuration.

that the removal of moisture does result in a higher reaction rate, but not significantly so when compared with the previous observations for the conventionally prepared Co_3O_4 nanoparticles^{12,13}.

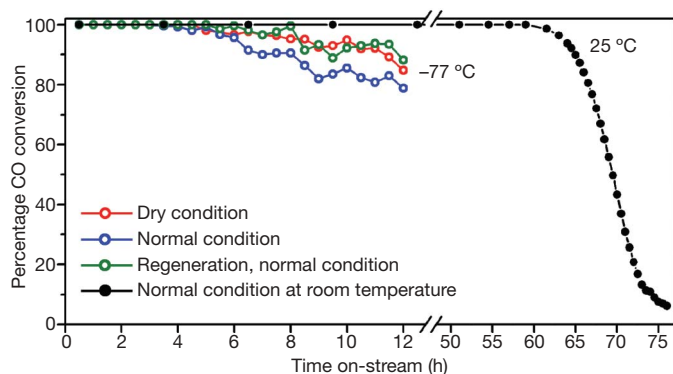


Figure 2 | Effects of moisture content, regeneration and temperature on the oxidation of CO over Co_3O_4 nanorods. CO oxidation with a feed gas of 1.0 vol.% CO/2.5 vol.% O_2 /He under normal (moisture 3–10 p.p.m., blue symbols) and dry (moisture <1 p.p.m., red symbols) conditions at -77°C . The used sample was regenerated with a 20 vol.% O_2 /He mixture at 450°C for 30 min and then tested for CO oxidation under normal conditions (green symbols) at -77°C . CO oxidation at 25°C (black symbols) was tested with the normal feed gas.

Co_3O_4 has a spinel structure containing Co^{3+} in an octahedral coordination and Co^{2+} in a tetrahedral coordination. The former is regarded as the active site for CO oxidation, whereas the latter is almost inactive^{18–20}. The redox cycle connecting the two stages is largely responsible for the successful CO oxidation. As shown in Fig. 3a, oxygen anions form a distorted face-centred cubic sublattice, in which Co^{2+} cations occupy one-eighth of the tetrahedral interstices and Co^{3+} cations occupy half of the octahedral interstices. The close-packed planes are $\{001\}$, $\{111\}$ and $\{110\}$, and their surface atomic configurations are illustrated in Fig. 3b–d. Clearly, the $\{001\}$ and $\{111\}$ planes contain only Co^{2+} cations, while the $\{110\}$ plane is composed mainly of Co^{3+} cations. In fact, surface differential diffraction studies have proved that the Co^{3+} cations are present solely on the $\{110\}$ plane^{21,22}. Therefore, it is most likely that CO oxidation on the Co_3O_4 nanorods follows the reaction pathway shown in Fig. 3e. The CO molecule interacts preferably with the surface Co^{3+} cation, which is the only favourable site for CO adsorption, as confirmed both theoretically²³ and experimentally^{13,24}. The oxidation of the adsorbed CO then occurs by abstracting the surface

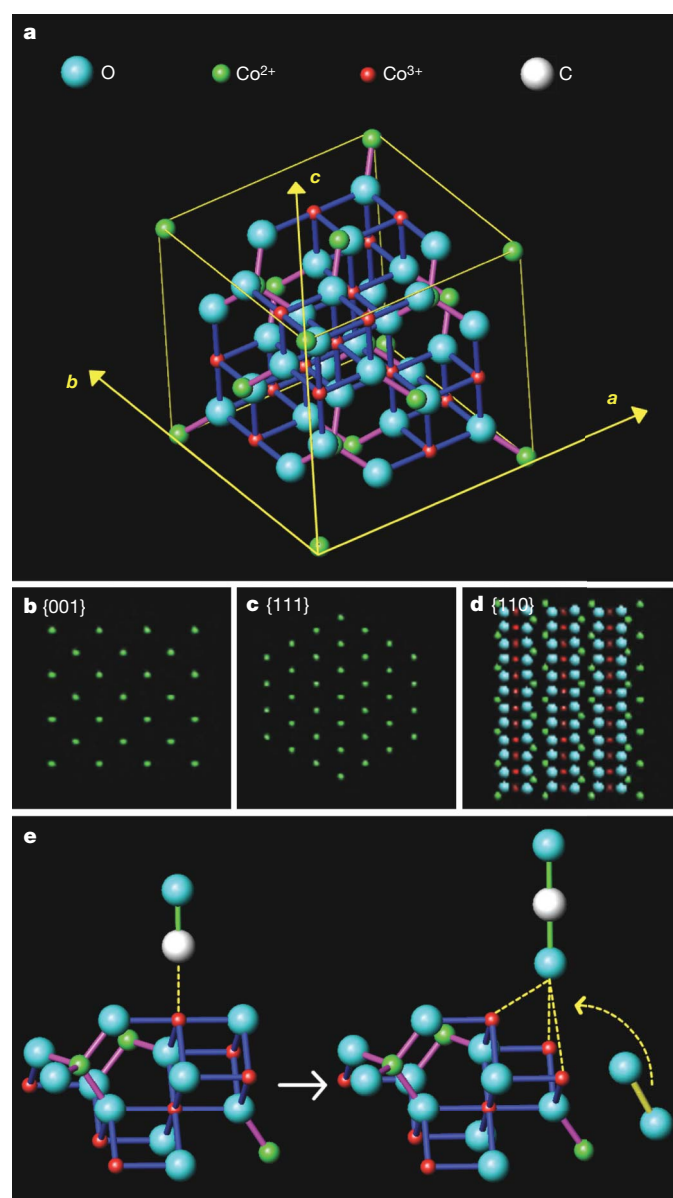


Figure 3 | Possible reaction pathway for CO oxidation on Co_3O_4 nanorod. **a**, Spinel structure of Co_3O_4 crystal. **b–d**, The surface atomic configurations in the $\{001\}$ (**b**), $\{111\}$ (**c**), and $\{110\}$ (**d**) planes. **e**, A ball-and-stick model for CO adsorption and oxidation on the active Co^{3+} site.

oxygen that might be coordinated with three Co^{3+} cations. Finally, the partially reduced cobalt site, which might be a Co^{2+} cation with a neighbouring oxygen vacancy, is re-oxidized by a gas-phase oxygen molecule to the active Co^{3+} site. The Co_3O_4 nanorod exposes four surface {110} planes that are rich in Co^{3+} sites, so we would expect it to exhibit a much higher activity for CO oxidation than the conventional nanoparticle, which exposes mainly the {001} and {111} planes (Supplementary Fig. S2), which contain only inactive Co^{2+} sites^{13,18}.

The reaction orders of CO and O_2 over the Co_3O_4 nanorods were 0.12 and 0.28 (Fig. 4a), respectively, suggesting that the surfaces of the nanorods are almost saturated with CO and O_2 , leading to very weak dependencies of the reaction rate on the gas-phase CO and O_2 concentrations. When the reaction temperature is far below room temperature, the rate of adsorption of reactant can usually exceed the rate of surface reaction. The abundant Co^{3+} cations on the {110} plane provides sufficient sites for CO adsorption, which occurs readily. The reaction between the adsorbed CO and the nearby oxygen species to form CO_2 seems to be the rate-determining step because the ensuing regeneration of the active oxygen site with a gas-phase oxygen molecule takes place rapidly through interactions with the partially reduced cobalt cations^{23,24}. As a result, CO oxidation could occur far below room temperature as long as both reactants are simultaneously present on the active surface.

The apparent activation energy of CO oxidation over the Co_3O_4 nanorods was 22 kJ mol^{-1} , which is almost the same as that of the Co_3O_4 nanoparticles (Fig. 4b). This implies that the active site for CO oxidation in both cases is identical and is Co^{3+} . Turnover frequencies estimated on the basis of the Co^{3+} site are essentially similar for the nanorods and the nanoparticles (Supplementary Table S1). The pre-exponential factor for the Co_3O_4 nanorods is $8.0 \times 10^{24} \text{ molecules g}^{-1} \text{ s}^{-1}$, whereas the corresponding value for the Co_3O_4 nanoparticles is only $5.7 \times 10^{23} \text{ molecules g}^{-1} \text{ s}^{-1}$. This strongly indicates that the difference in the reaction rate is due solely to the variation in the number of active sites and that the significantly higher reaction rate of the nanorods can be ascribed to the richness in active Co^{3+} sites on the surfaces through preferentially exposing the reactive {110} planes.

To identify the reason for the gradual deactivation of the Co_3O_4 nanorods during the course of the reaction at -77°C with the normal feed gas, a deactivated sample was treated with a 20 vol.% O_2/He mixture at 450°C , through which the deposited carbonates and/or bicarbonates and $\text{H}_2\text{O}/\text{OH}^-$ species are completely desorbed as water and CO_2 (Supplementary Fig. S3). When exposed to the reaction gas again at -77°C , the regenerated sample exhibited fully recovered and even better activity for CO oxidation (Fig. 2). Hence, the loss in activity

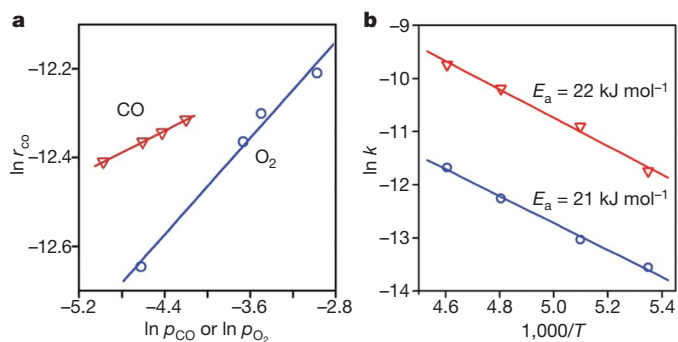


Figure 4 | Reaction kinetics of CO oxidation. **a**, Reaction rates (r_{CO}) as a function of CO or O_2 concentration over Co_3O_4 nanorods: (triangle symbols) CO and (circle symbols) O_2 . The reaction rates were measured at -77°C and the concentrations of CO and O_2 were in the ranges of 0.5–1.2 vol.% and 1.0–5.1 vol.%, respectively. p_{CO} , p_{O_2} , partial pressures. **b**, Arrhenius plots for the reaction rate constants (activation energies, E_a) on Co_3O_4 nanorods (triangle symbols) and nanoparticles (circle symbols) in the temperature (T) range of -86 to -56°C with a feed gas of 1.0 vol.% CO/2.5 vol.% O_2/He .

during CO oxidation can be ascribed to the accumulation of carbonates and/or bicarbonates and $\text{H}_2\text{O}/\text{OH}^-$ species on the surfaces of the nanorods, which gradually hinder the adsorption of CO and oxygen.

The Co_3O_4 nanorods were further tested for CO oxidation in the normal feed gas at temperatures close to those of practical applications. The reaction at room temperature gave 100% CO conversion for about 65 h owing to the limited accumulation of carbonates and $\text{H}_2\text{O}/\text{OH}^-$ species (Fig. 2). Subsequent regenerations of up to ten cycles showed that the Co_3O_4 nanorods gradually stabilized their high activity with 100% CO conversion for about 60 h, clearly indicating that the Co_3O_4 nanorods can easily catalyse CO oxidation at ambient temperature with sustainable durability.

The Co_3O_4 nanorods were also examined for the oxidation of CO and propane in feed streams containing large amounts of H_2O and CO_2 (Supplementary Fig. S4), similar to automotive exhaust gas composition²⁵. The conversion of CO was 100% at 200°C under stoichiometric conditions and in the presence of water. The coexistence of H_2O , CO_2 and C_3H_8 in the feed gas marginally lowered the conversion of CO (to $\sim 96\%$) at 200°C , suggesting that CO oxidation takes place preferentially over propane oxidation. The lower CO conversion ($\sim 40\%$) at 150°C might be caused by the deposition of carbonates, which tends to occur at such a low temperature and with less O_2 present. When a stoichiometric amount of O_2 for the combustion of both CO and propane was present in the feed stream, the conversion of CO reached 100% at 200°C , but only a trace amount of propane was oxidized to CO_2 and H_2O . The conversion of propane to CO_2 and H_2O reached 100% at 350°C , demonstrating that the oxidation ability of the Co_3O_4 nanorods for propane is at least comparable to that of Pt and Pd catalysts^{2,26}. This observation is in accord with the general understanding that CO is preferentially oxidized at low temperatures, whereas as the temperature is increased propane is gradually oxidized^{2,25}.

TEM observations of the samples used for the above catalytic tests proved that the nanorod-shaped structure is still well maintained (Supplementary Fig. S5), confirming the high thermal stability of the Co_3O_4 nanorods even in the presence of large amounts of H_2O and CO_2 . Hence, the Co_3O_4 nanorods presented here not only display high activities for the oxidation of CO and propane in the automotive exhaust at low temperatures but also meet the most essential requirement: thermal stability under practical conditions.

In conclusion, we have demonstrated that morphological control of Co_3O_4 is very rewarding: the nanorods not only exhibit surprisingly high catalytic activity for CO oxidation at temperatures as low as -77°C but are also sufficiently stable in feed gases containing large amounts of H_2O and CO_2 at 200 – 400°C . This fundamental understanding shows that morphological control of base transition-metal oxides allows preferential exposure of catalytically active sites, and will most probably be applicable in the development of the next generation of highly efficient oxidation catalysts.

METHODS SUMMARY

Co_3O_4 nanorods. 4.98 g of cobalt acetate tetrahydrate was dissolved in 60 ml of ethylene glycol and the mixture was gradually heated to 160°C . 200 ml of aqueous 0.2 M Na_2CO_3 solution was then added and the slurry was further aged for 1 h under vigorous stirring and a continuous flow of nitrogen. After filtration and being washed with water, the solid obtained was dried at 50°C overnight under vacuum and calcined at 450°C for 4 h in air.

Structural analysis. TEM images of the samples were recorded on a Philips Tecanai F 30 G² microscope. The specimen was prepared by ultrasonically suspending the Co_3O_4 powder in ethanol. A drop of the suspension was deposited on a carbon-enhanced copper grid and dried in air.

Catalytic evaluation. The CO oxidation reaction was performed in a continuous-flow fixed-bed quartz reactor under atmospheric pressure. 200 mg (40–60 mesh) sample was loaded and pre-treated with a 20 vol.% O_2/He mixture (50 ml min^{-1}) at 450°C for 30 min. After cooling to -77°C , a 1.0 vol.% $\text{CO}/2.5 \text{ vol.}\% \text{ O}_2/\text{He}$ mixture (50 ml min^{-1}) was introduced. Dry conditions were obtained by passing the feed gas through a molecular-sieve trap cooled to dry-ice temperature. Kinetic measurements were conducted at -86 to -56°C with feed streams of 0.5–1.2 vol.% CO and 1.0–5.1 vol.% O_2 balanced with He, and the CO conversions were adjusted

to below 15% by varying the hourly gas space velocity to calculate the reaction rates under differential reactor conditions. The amounts of CO, CO₂ and O₂ in the inlet and outlet streams were measured by an on-line gas chromatograph.

Received 9 December 2007; accepted 16 February 2009.

- Shelief, M. & McCabe, R. W. Twenty-five years after introduction of automotive catalysts: what next? *Catal. Today* **62**, 35–50 (2000).
- Twigg, M. V. Progress and future challenges in controlling automotive exhaust gas emissions. *Appl. Catal. B* **70**, 2–15 (2007).
- Merrill, D. R. & Scalione, C. C. The catalytic oxidation of carbon monoxide at ordinary temperatures. *J. Am. Chem. Soc.* **43**, 1982–2002 (1921).
- Yoon, C. & Cocke, D. L. The design and preparation of planar models of oxidation catalysts: I. Hopcalite. *J. Catal.* **113**, 267–280 (1988).
- Trimm, D. L. & Onsan, Z. I. Onboard fuel conversion for hydrogen-fuel-cell-driven vehicles. *Catal. Rev. Sci. Eng.* **43**, 31–84 (2001).
- Oh, S. H. & Hoflund, G. B. Low-temperature catalytic carbon monoxide oxidation over hydrous and anhydrous palladium oxide powders. *J. Catal.* **245**, 35–44 (2007).
- Date, M., Okumura, M., Tsubota, S. & Haruta, M. Vital role of moisture in the catalytic activity of supported gold nanoparticles. *Angew. Chem. Int. Edn Engl.* **43**, 2129–2132 (2004).
- Haruta, M., Kobayashi, T., Sano, H. & Yamada, N. Novel gold catalysts for the oxidation of carbon monoxide at a temperature far below 0 °C. *Chem. Lett.* **16**, 405–408 (1987).
- Haruta, M. *et al.* Low-temperature oxidation of CO over gold supported on TiO₂, α-Fe₂O₃ and Co₃O₄. *J. Catal.* **144**, 175–192 (1993).
- Yao, Y. Y. The oxidation of hydrocarbons and CO over metal oxides. III. Co₃O₄. *J. Catal.* **33**, 108–122 (1974).
- Perti, D. & Kabel, R. L. Kinetics of CO oxidation over Co₃O₄/Al₂O₃. *AIChE J.* **31**, 1420–1440 (1985).
- Cunningham, D. A. H., Kobayashi, T., Kamijo, N. & Haruta, M. Influence of dry operating conditions: observation of oscillations and low temperature CO oxidation over Co₃O₄ and Au/Co₃O₄ catalysts. *Catal. Lett.* **25**, 257–264 (1994).
- Grillo, F., Natile, M. M. & Glisenti, A. Low-temperature oxidation of carbon monoxide: the influence of water and oxygen on the reactivity of a Co₃O₄ powder surface. *Appl. Catal. B* **48**, 267–274 (2004).
- Thormählen, P., Skoglundh, M., Fridell, E. & Andersson, B. Low-temperature CO oxidation over platinum and cobalt oxide catalysts. *J. Catal.* **188**, 300–310 (1999).
- Saalfrank, J. W. & Maier, W. F. Directed evolution of noble-metal-free catalysts for the oxidation of CO at room temperature. *Angew. Chem. Int. Edn Engl.* **43**, 2028–2031 (2004).
- Fortunato, G., Oswald, H. R. & Reller, A. Spinel-oxide catalysts for low temperature CO oxidation generated by use of an ultrasonic aerosol pyrolysis process. *J. Mater. Chem.* **11**, 905–911 (2001).
- Szegedi, Á., Hegedüs, M., Margitfalvi, J. L. & Kiricsi, I. Low-temperature CO oxidation over iron-containing MCM-41 catalysts. *Chem. Commun.* 1441–1443 (2005).
- Petitto, S. C., Marsh, E. M., Carson, G. A. & Langell, M. A. Cobalt oxide surface chemistry: the interaction of CoO (100), Co₃O₄ (110) and Co₃O₄ (111) with oxygen and water. *J. Mol. Catal. A* **281**, 49–58 (2008).
- Jansson, J. *et al.* On the catalytic activity of Co₃O₄ in low-temperature CO oxidation. *J. Catal.* **211**, 387–397 (2002).
- Omata, K., Takada, T., Kasahara, S. & Yamada, M. Active site of substituted cobalt spinel oxide for selective oxidation of CO/H₂. Part II. *Appl. Catal. A* **146**, 255–267 (1996).
- Beaufils, J. P. & Barbaux, Y. Study of adsorption on powders by surface differential diffraction measurements. Argon on Co₃O₄. *J. Appl. Cryst.* **15**, 301–307 (1982).
- Ziólkowski, J. & Barbaux, Y. Identification of sites active in oxidation of butene-1 to butadiene and CO₂ on Co₃O₄ in terms of the crystallochemical model of solid surfaces. *J. Mol. Catal.* **67**, 199–215 (1991).
- Broqvist, P., Panas, I. & Persson, H. A. DFT study on CO oxidation over Co₃O₄. *J. Catal.* **210**, 198–206 (2002).
- Jansson, J. Low-temperature CO oxidation over Co₃O₄/Al₂O₃. *J. Catal.* **194**, 55–60 (2000).
- Heck, R. M. & Farrauto, R. J. Automobile exhaust catalysts. *Appl. Catal. A* **221**, 443–457 (2001).
- Sharma, S., Hegde, M. S., Das, R. N. & Pandey, M. Hydrocarbon oxidation and three-way catalytic activity on a single step directly coated cordierite monolith: High catalytic activity of Ce_{0.98}Pd_{0.02}O_{2–δ}. *Appl. Catal. A* **337**, 130–137 (2008).

Supplementary Information is linked to the online version of the paper at www.nature.com/nature.

Acknowledgements We thank C. Li, L. Lin and X. Bao of the Dalian Institute of Chemical Physics, Chinese Academy of Sciences, for their encouragement and discussions. We also acknowledge financial supports for this research work from the National Natural Science Foundation of China and the National Basic Research Program of China.

Author Contributions X.X. and Y.L. performed the synthesis of Co₃O₄ nanorods/nanoparticles and the catalytic tests. Z.-Q.L. conducted the transmission electron microscopy observations and structural analysis. M.H. and W.S. designed the study, analysed the data and wrote the paper. All authors discussed the results and commented on the manuscript.

Author Information Reprints and permissions information is available at www.nature.com/reprints. Correspondence and requests for materials should be addressed to W.S. (shen98@dicp.ac.cn).